Food Bioprocess Technol (2013) 6:2571–2585
DOI 10.1007/s11947-012-0895-5

COMMUNICATION

Investigating the Effects of Table Grape Package Components and Stacking on Airflow, Heat and Mass Transfer Using 3-D CFD Modelling

Mulugeta A. Delele · Mduduzi E. K. Ngcobo · Umezuruike Linus Opara · Chris J. Meyer

Received: 30 September 2011 / Accepted: 15 May 2012 / Published online: 30 May 2012

Abstract The flow phenomenon during cooling and handling of packed table grapes was studied using a computational fluid dynamic (CFD) model and validated using experimental results. The effects of the packaging components (bunch carry bag and plastic liners) and box stacking on airflow, heat and mass transfer were analysed. The carton box was explicitly modelled, grape bunch with the carry bag was treated as a porous medium and perforated plastic liners were taken as a porous jump. Pressure loss coefficients of grape bunch with the carry bag and perforated plastic liners were determined using wind tunnel experiments. Compared with the cooling of bulk grape bunch, the presence of the carry bag increased the half and seven eighth cooling time by 61.09 and 97.34 %, respectively. The addition of plastic liners over the bunch carry bag increased the half and seven eighth cooling time by up to 168.90 and 185.22 %, respectively. Non-perforated liners were most effective in preventing moisture loss but also generated the highest condensation of water vapour inside the package. For perforated plastic liners, cooling with a high relative humidity (RH) air minimised fruit moisture loss. Partial cooling of the grape bunch inside the carry bag before covering it with a non-perforated plastic liner maintained the required high RH inside the package without condensation. The stacking of packages over the pallet affected the airflow pattern, the cooling rate and moisture transfer. There was a good agreement between measured and predicted results. The result demonstrated clearly the applicability of CFD models to determine optimum table grape packaging and cooling procedures.

Keywords Table grape · Packaging · CFD · Airflow · Heat and mass transfer · Plastic liner

M. A. Delele · M. E. K. Ngcobo · U. L. Opara (✉)
Postharvest Technology Research Laboratory,
South African Research Chair in Postharvest Technology,
University of Stellenbosch,
Private Bag X1, Matieland,
7602 Stellenbosch, South Africa
e-mail: opara@sun.ac.za

C. J. Meyer
Department of Mechanical and Mechatronics Engineering,
Faculty of Engineering, University of Stellenbosch,
Private Bag X1, Matieland,
7602 Stellenbosch, South Africa

M. E. K. Ngcobo
Perishable Products Export Control Board,
45 Silwerboom Avenue, Platterkloof,
Parow 7500, South Africa

Notation

A_c	Cooler surface area (m^2)
a_p	Specific fruit area (m^{-1})
Bi	Biot number
C_p	Specific heat capacity (J kg^{-1} $°C^{-1}$)
D	Diffusion coefficient (m^2 s^{-1})
D_c	Collar diameter of heat exchanger tube (m)
D_e	Effective diffusivity (m^2 s^{-1})
D_P	Fruit diameter (m)
g	Gravitational acceleration (m s^{-2})
h_h	Heat transfer coefficient (W m^{-2} $°C^{-1}$)
h_m	Mass transfer coefficient (m s^{-1})
K	Darcy permeability (m^2)
k	Turbulence kinetic energy (m^2 s^{-2})
L	Latent heat (J kg^{-1})
p	Pressure (Pa)
Pr	Prandtl number
p_{sat}	Saturated vapour pressure (Pa)
p_v	Vapour pressure (Pa)
Re	Reynolds number

Sc	Schmidt number
S_e	Heat source term (W m^{-3})
S_m	Mass source term (kg m^{-3} s^{-1})
St	Stanton number
t	Time (s)
T	Temperature (°C)
T'	Fluctuating temperature (°C)
u_i, u_j	Mean velocity components in X, Y, and Z directions (m s^{-1})
u_i', u_j'	Fluctuating velocity components (m s^{-1})
V	Volume (m^{-3})
x_i, x_j	Cartesian coordinates (m)
X_v	Moisture content (kg/kg)
Y_v	Vapour mass fraction
β	Forchheimer drag coefficient (m^{-1})
ε	Dissipation rate of turbulence kinetic energy (m^2 s^{-3})
μ	Dynamic viscosity (kg m^{-1} s^{-1})
λ	Thermal conductivity (W m^{-1} °C^{-1})
ω	Specific dissipation rate (s^{-1})
ρ	Density (kg m^{-3})
ϕ	Porosity
α	Thermal expansion coefficient (°C^{-1})

Subscripts

a	Air phase
c	Cooler
o	Reference condition
p	Product
t	Turbulence
i, j	Cartesian coordinate index

Introduction

Fresh table grape is a major commodity in global food trade, and South Africa is ranked third in the world export market, with the European market accounting for about 61 % of the total export (Ngcobo et al. 2011). Packaging and refrigerated storage are critical technologies in maintaining quality of fresh and processed food products (de Paula et al. 2011; Opara 2011; Caleb et al. 2011; Tsiraki and Savvaidis 2011). For fresh table grape export, produce is typically packed in 4.5 kg vented cardboard boxes with multiple inner packaging materials that include plastic liner, SO_2 pad, moisture absorber and bunch carry bag (Fig. 1). The main function of these package components are to maintain the quality of the grape during postharvest handling and storage by providing a mechanical shield against injuries, minimising product moisture loss and retarding microbial decay (Opara 2011). Produce temperature

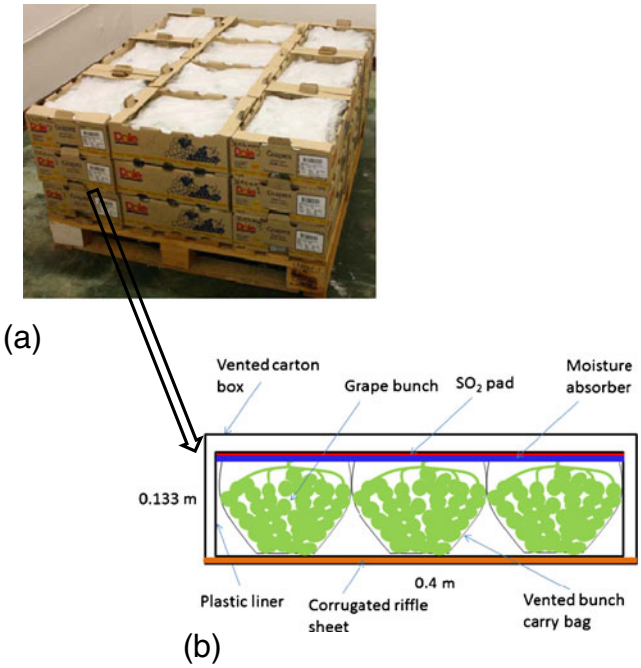

Fig. 1 Table grape package: **a** picture of packed table grape and **b** diagram showing the details inside a packed box

is one of the most important parameters that control the rate of respiration, moisture loss and microbial growth. Cooling of table grape as fast as possible retards quality deteriorations associated with these phenomena. Table grape is a non-climacteric fruit with a relatively low postharvest physiological activity; however, unless the appropriate measures are taken to maintain the cold chain, produce may be exposed to high levels of moisture loss and decay (Nelson 1985; Lichter et al. 2008; Costa et al. 2011; Ngcobo et al. 2011). Moisture loss results in quality problems such as weight loss, stem drying, browning, softening and shattering of berries which contribute to significant economic losses.

The cooling of packed table grapes is usually performed using a forced air cooling technique. Due to the high vapour pressure difference between the cooling air and the product surface, the initial cooling period of the produce from its field temperature to the desired storage temperature is usually associated with significant moisture loss (Nelson 1978; Lichter et al. 2011). Crisosto et al. (2001) observed up to 1 % moisture loss during the cooling period of table grapes. Although this level of moisture loss is considered small, the authors noted that it caused stem browning. Lowering the vapour pressure difference as fast as possible either by decreasing the berry temperature or increasing the relative humidity (RH) of air can minimise moisture loss. Berry cooling rate depends on several factors including box vent area (Opara 2011), cooling air properties (flow rate, temperature

and RH), stacking pattern, liner properties and the presence of other components inside the package (such as moisture absorption pad and SO_2 pad). The properties of the liner include plastic type and vent size, number and distribution. Previous researchers have shown that the presence of packing materials and cooling duration significantly influence/alter the decay of grape berries (Nelson and Ahmedullah 1976; Nelson 1978). Therefore, fresh produce package must have enough vents to allow the delivery of the cooling medium (air) with minimum resistance and provide uniform airflow and cooling through the entire mass of the produce while providing suitable mechanical resistance (Vigneault and Goyette 2002; Castro et al. 2004; Vigneault and Castro 2005). Plastic liners are used in table grape packaging to minimise moisture loss from berries by maintaining high RH within the package. Recent experimental studies showed that non-perforated plastic liners maintained the RH of the package close to 100 % resulting in the highest stem quality (Ngcobo et al. 2011). However, the use of non-perforated plastic liner also produced the highest moisture condensation inside the package, SO_2 injury and berry drop while the use of perforated liners resulted in lower RH, higher stem dehydration and browning compared with the non-perforated liner. These findings highlight the need for optimisation of plastic liner designs.

The airflow, heat and mass transfer processes during postharvest handling of horticultural products have been studied using experimental and modelling techniques (Tassou and Xiang 1998; Xu and Burfoot 1999; Alvarez and Flick 1999; van der Sman 2002; Alvarez et al. 2003; Moureh and Flick 2004; Nahor et al. 2005; Zou et al. 2006; Opara and Zou 2006, 2007; Chourasia and Goswami 2007; Delele et al. 2009a, b; Ferrua and Singh 2009; Tutar et al. 2009). Some researchers have studied the airflow, heat and mass transfer processes within the individual and packed grapes using experimental (Gentry and Nelson 1964; Nelson 1978; Frederick and Comunian 1994) and modelling techniques (Dincer 1995a, b; Acevedo et al. 2007). However, none of the previous studies have developed a comprehensive 3-D computational fluid dynamic (CFD) model which is capable of predicting the airflow, heat and mass transfer within and around multiple package components such as that used for fresh table grapes (Fig. 1). These studies did not take into account the details of the packages and even the grape bunches. For better understanding of the flow behaviour in and around such complex packaging systems, the development of better modelling techniques is vital. Nowadays, the use of validated CFD modelling technique has increasingly become an alternative approach to the difficult, time consuming and expensive experimental methods (Delele et al. 2009a; Tutar et al. 2009; Opara 2011).

The aim of this study was to develop and experimentally validate a 3-D CFD model of table grape cooling process that predicted the cooling air velocity, temperature, RH and product moisture loss, taking into account the detailed geometries of the packaging components (box, liner and pads). The validated model was used to evaluate the effect of different package components and cooling procedures on airflow, heat and mass transfer processes.

Materials and Methods

Cold Storage Room and Table Grape Package

The study was based on an experimental cold storage room with dimensions 3.05×2.40×2.83 m (Fig. 2). The room is equipped with three fans of 30-cm diameter that circulate the cooling air through the cooler and the room. The capacity of each fan is 1,290 m^3/h, and the cooling unit is composed of finned tube heat exchanger with dimensions of 1.25×0.40×0.36 m.

Grape bunches were packed using vented carton box with dimensions of 0.4 m long, 0.3 m wide and 0.133 m high (Fig. 1). Every box contains about 4.5 kg of grape; equivalent to six to eight bunches depending on the size of the grape bunch. The carry bags were well vented. During packing, each carry bag containing a bunch of berries is placed inside the plastic liner, the moisture absorption and SO_2 pads are placed over the carry bags and the liner is closed and sealed using a plastic tape. A corrugated paperboard sheet is placed at the

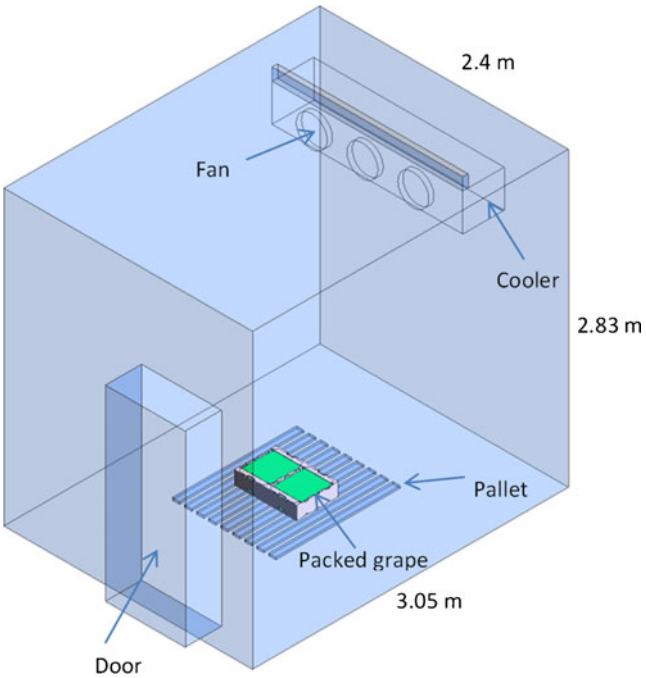

Fig. 2 Details of the experimental cold storage room

bottom of the box to protect the berries against bruising. More detailed description of the table grape packaging system can be found in Ngcobo et al. (2011).

CFD Model Formulation

The CFD code used for this work was ANSYS FLUENT 13.0 (ANSYS, Inc., Canonsburg, PA, USA). The governing equations were solved using Reynolds-averaged procedure. In Cartesian coordinates, for flow in a porous medium, the Reynolds-averaged fluid flow equations based on interstitial fluid velocity are as follows (Antohe and Lage 1997; Nakayama and Kuwahara 1999):

$$\frac{\partial(\rho_a)}{\partial t}+\frac{\partial(\rho_a u_i)}{\partial x_i}=S_{\mathrm{m}} \tag{1}$$

$$\begin{aligned}\frac{\partial(\rho_a u_i)}{\partial t}+\frac{\partial\left(\rho_a u_i u_j\right)}{\partial x_j}=&-\frac{\partial(p)}{\partial x_i}+\frac{\partial}{\partial x_j}\left[\mu_a\left(\frac{\partial u_i}{\partial x_j}+\frac{\partial u_j}{\partial x_i}\right)\right]-\frac{\partial}{\partial x_j}\left(\rho_a\overline{u'_i u'_j}\right)\\&-[1-\alpha(T-T_o)]\rho_a g-\phi\frac{\mu_a}{K}u_i-\phi^2\frac{1}{2}\beta\rho_a\left(u_j u_j\right)^{1/2}u_i\end{aligned} \tag{2}$$

where ρ_a is the density (in kilogrammes per cubic metre); u_i and u_j are air velocity components (in metres per second); t is the time (in seconds); x_i and x_j are Cartesian coordinates (in metres); p is the pressure (in pascals); μ_a is the dynamic viscosity (in kilogrammes per metre per second); u_i' and u_j' are fluctuating velocity components (in metres per second); T is the temperature (in degrees Celsius); ϕ is the porosity; g is the gravitational acceleration (in metres per second); α is the thermal expansion coefficient (in degrees Celsius); and S_{m} is the mass source term (in kilogrammes per metre per second). The fourth term in the right side of Eq. 2 represents the buoyancy force, where the reference temperature (T_o) was taken as the storage room temperature. The last two terms in the right side of Eq. 2 represent the resistance of the porous medium to airflow and expressed in the form of Darcy–Forchheimer equation; where K is the Darcy permeability (in square metres) and β is the Forchheimer drag coefficient (in metres).

By assuming a local thermal equilibrium between the air and the porous solid matrix, the energy equation is:

$$\begin{aligned}\frac{\partial}{\partial t}\left(\phi\rho_a C_{pa}T+(1-\phi)\rho_p C_{pp}T\right)+\frac{\partial}{x_j}\left(\phi\rho_a C_{pa}u_j T\right)=&\frac{\partial}{\partial x_j}\left[\lambda_e\left(\frac{\partial T}{\partial x_j}\right)\right]\\&-\frac{\partial}{\partial x_j}\left(\phi\rho_a C_{pa}\overline{u'_j T'}\right)+S_e\end{aligned} \tag{3}$$

Where C_P is the heat capacity (in Joules per kilogramme per degrees Celsius); λ_e is the effective thermal conductivity (in watts per metre per degrees Celsius); T' is the fluctuating temperature (in degrees Celsius); and S_e is the energy source term (in watts per cubic metre). The Effective thermal conductivity was estimated using: $\lambda_{\mathrm{eff}}=\phi\lambda_a+(1-\phi)\lambda_p$(Carson 2006). The limitation of this thermal equilibrium assumption for porous systems with heat generation and transient problems, particularly for large products and low conductivity fluid has been discussed (Verboven et al. 2006; van der Sman 2008; Laguerre et al. 2008). During such non-equilibrium cases, a two-equation model is recommended. However, thermal equilibrium assumption has been used and reasonable model accuracy was reported in several heat and mass transfer studies related to agricultural product handling (Tassou and Xiang 1998; Moureh and Flick 2004; Chourasia and Goswami 2007; Delele et al. 2009a, b, 2012). Using scale analysis, van der Sman (2008) reported that this thermal equilibrium assumption is valid when the air Stanton number, $\mathrm{St}_a=\frac{L_x h_h a_p}{u_x\rho_a C_{pa}}\gg 1$, vapour Stanton number, $\mathrm{St}_v=\frac{L_x h_m a_p}{u_x}\approx 1$, Biot number, $\mathrm{Bi}=\frac{h_h D_p}{\lambda_p}\ll 1$ and the particle Reynolds number, $Re_p=\frac{\rho_a u_x D_p}{\mu_a}<10^3$. The initial temperature of the grape was 21 °C, and the cooling air temperature was 0 °C. Density, specific heat and thermal conductivity of the grapes were 1,077.9 kg m^{-3}, 3,395 Jkg^{-1} $^{\circ}\mathrm{C}^{-1}$ and 0.551 Wm^{-} $^{\circ}\mathrm{C}^{-1}$, respectively (Bingol et al. 2008). Corresponding values of the cooling air were 1.25 kg m^{-3}, 1,005 Jkg^{-1} $^{\circ}\mathrm{C}^{-1}$ and 0.024 Wm^{-1} °C. Length of the porous region (L_x) was 0.4 m, average diameter of the grapes (D_p) was 0.0201 m

and calculated average air velocity inside the bulk grape region (u_x) was 0.059 $m s^{-1}$. Porosity of the grapes was determined by using displacement method (Chau et al. 1985) and it was 0.53. The specific grape area (a_p) was 158.21 m^{-1}. Correlations to determine the heat transfer coefficient (h_h) in packed beds can be found in Wakao and Kaguei (1982) and van der Sman (2008). Using this correlation, the calculated value of h_h was 9.78 $W m^{-2} \circ C^{-1}$. Mass transfer coefficient (h_m) of table grape takes into account convective mass transfer coefficient (h_{ma}) and skin mass transfer coefficient (h_{ms}), $\frac{1}{h_m} = \frac{1}{h_{ma}} + \frac{1}{h_{ms}}$. The convective mass transfer coefficient was determined from the heat transfer coefficient using Lewis analogy (Bird et al. 2002). Table grape skin mass transfer coefficient was taken from Becker et al. (1994). The calculated value of h_m was 8.23×10^{-4} m s^{-1}, and the calculated values of St_a, St_v, Bi and Re_p were 8.31, 0.87, 0.35 and 83.28, respectively. In this study, Bi value was close to 1. However, the agreement between measured and predicted results (see 'Cooling Airflow and Temperature Distribution' and 'Effect of Package Components on Heat and Mass Transfer During Cooling and Storage') shows the validity of the thermal equilibrium assumption.

The transport equation for vapour mass fraction is:

$$\frac{\partial(\phi\rho_a Y_v)}{\partial t} + \frac{\partial}{\partial x_j}\left(\phi\rho_a u_j Y_v\right) = \frac{\partial}{\partial x_j}\left[\rho_a D_e\left(\frac{\partial(Y_v)}{\partial x_j}\right)\right] - \frac{\partial}{\partial x_j}\left(\phi\rho_a \overline{u'_j Y_v'}\right) + S_m \quad (4)$$

Where Y_v is the vapour mass fraction; Y_v' is the fluctuating vapour mass fraction and D_e is the effective diffusivity of the vapour (in cubic metres per second). The specific Reynolds stress term ($\overline{u'_i u'_j}$) in Eq. 2 and specific Reynolds flux terms $\overline{u'_j T'}$ and $\overline{u'_j Y'_v}$ in Eqs. 3 and 4, respectively were approximated by (Versteeg and Malalasekera 1995; Wilcox 2000):

$$\overline{u'_i u'_j} = -\frac{\mu_t}{\rho_a}\left(\frac{\partial u_i}{\partial x_j} + \frac{\partial u_j}{\partial x_i}\right) + \frac{2}{3}k\delta_{ij} \quad (5)$$

$$\overline{u'_j T'} = -\frac{\mu_t}{\rho_a \mathrm{Pr}_t}\left(\frac{\partial T}{\partial x_j}\right) \quad (6)$$

$$\overline{u'_j Y'_v} = -\frac{\mu_t}{\rho_a \mathrm{Sc}_t}\left(\frac{\partial Y_v}{\partial x_j}\right) \quad (7)$$

Appropriate turbulence models were used for closure of these equations. The Reynolds stress term (Eq. 5) is commonly treated using Boussinesq hypothesis. This hypothesis relates the Reynolds stress term to the mean velocity gradient and assumes the turbulent viscosity to be isotropic scalar quantity, which is not strictly true. The Boussinesq hypothesis is used in Spalart–Allmaras, $k-\varepsilon$, and $k-\omega$ turbulence models. The Reynolds stress turbulence model is an alternative approach that takes into account the anisotropy of the Reynolds stress term, but with additional computational cost. In most applications, models based on Boussinesq hypothesis perform very well (Wilcox 2000; Ansys 2010). Alvarez and Flick (1999) observed turbulence generation behind the stacked product and later Alvarez et al. (2003) proposed a semi-empirical model based on one equation for two-dimensional turbulence flow through porous medium that took into account this turbulence generation. Though the generation of turbulence behind the stacked product was reported (Alvarez and Flick 1999; Alvarez et al. 2003), several previous studies on airflow, heat and mass transfer in loaded refrigerated systems used the porous medium approach and treated turbulence using conventional turbulence models that are employed in Reynolds-average approach (standard, $k-\varepsilon$; RNG, $k-\varepsilon$; SST, $k-\omega$; and Reynolds stress) (Hoang et al. 2000; Moureh and Flick 2004; Nahor et al. 2005; Mirade and Picgirard 2006; Delele et al. 2009a, b). Generally, the accuracy of these models was reasonable. In this study, different two-equation eddy-viscosity turbulence models (standard, $k-\varepsilon$; RNG, $k-\varepsilon$; standard, $k-\omega$; and SST, $k-\omega$) were compared. For standard ($k-\varepsilon$), RNG ($k-\varepsilon$), standard ($k-\omega$) and SST ($k-\omega$) turbulence models, the overall average relative error of predicted product temperature relative to the measured values was 23.94, 20.34, 21.85 and 17.13 % (see 'Cooling Airflow and Temperature Distribution'), respectively. The SST ($k-\omega$) turbulence model was chosen and used in this study.

The grape bunch with the carry bag and the cooler were modelled as a porous medium with the corresponding mass, momentum and heat sources/sink. The porous medium model describes the flow behaviour within a matrix of solid structure that is usually characterised by its porosity. As a result of the low Reynolds number (Re=83.28), the flow inside the liner (the grape bunch with the carry bag) was taken as a laminar flow. In all other regions the flow was turbulent. The source terms in Eqs. 1 and 2 consisted of different contributions. S_m takes into account the moisture loss from the product surface (S_{mp}) and the condensation of water vapour on the cooling coils (S_{mc}). S_e represents the heat of respiration of the product (S_{ep}) and the heat exchange on the cooler (S_{ec}). Due to the relatively low temperature difference between the surfaces, the effect of radiation was neglected. The details about the calculations of these source terms are given in 'Model Parameters Determination'. The model consisted of the following four zones: solid box zone, product zone, cooler zone and free air zone. In all zones, in addition to the relevant source

terms, the above equations were solved using the appropriate porosities. In the solid box zone, all source terms and porosity were zero and only heat transfer equation (Eq. 3) was solved. The product zone represented the region occupied by the grape bunch and the carry bag. In this zone, continuity, momentum, energy and vapour transport equations were solved. This zone included heat of respiration and product moisture loss as source terms and the porosity was taken as 0.53. The cooler zone represented the volume occupied by the cooler. The equations that were solved in the product zone were also solved here. Condensation of water vapour and heat exchange on the cooler were taken into account as source terms and the porosity was taken as 0.71. The free air zone consisted of the region that is not included in solid box, product and cooler zones. Similar to the product and cooler zones, Eqs. 1–4 were solved. In this zone, the porosity and the sources terms were taken as 1 and zero, respectively.

Model Parameters Determination

Bulk grape bunch was treated as a porous medium and vented plastic liner was modelled with porous jump boundary condition. Pressure loss coefficients were determined from experiments conducted in a wind tunnel (Fig. 3). The dimensions of the test section were 0.6 m in width (perpendicular to airflow), 0.4 m in height and 0.4 m in depth (in the airflow direction). The required airflow was attained using a suction fan. Independent pressure drop experiments were conducted for flow through bulk grape bunch which was uncovered with carry bag (Fig. 3b), bulk grape bunch which was covered with carry bag (Fig. 3c) and vented plastic liner (Fig. 3d). To measure the pressure drop through the bulk grape bunches with and without carry bag, the load was contained in a wire mesh and placed inside the wind tunnel. The pressure drop through the wire mesh was measured using a pressure transducer device (PMD70-AAA7-D22AAU, ENDRESS+HAUSER, Weil am Rhein, Germany) and was found to be close to zero. Measurements were done for fan frequency of 1 to 50 Hz; these frequencies corresponded to air velocity of 0.064 to 3.21 ms^{-1} for an empty wind tunnel.

For the porous bulk grape bunch, measured pressure drop value was expressed as function of air velocity and fitted to Darcy–Forchheimer equation ($\frac{\Delta P}{L_b} = -\frac{\mu}{K}u - \beta\frac{1}{2}\rho u^2$) with $r^2 \geq 0.993$ using Microsoft Excel solver. The solver determined the best fit by minimising the deviation between measured and predicted values. From the fitted equations, the values of the Darcy permeability (K) and Forchheimer drag coefficient (β) were determined. The first term in the right side of the equation is the Darcy term that accounts for the viscous drag which is dominant at low air velocities (laminar flow), while the second term is the Forchheimer term that accounts for the inertial drag which dominates the pressure drop at high air velocities (turbulent flow). Lb is the bulk length in the flow direction (0.4 m). In the case of bulk without carry bag, the measured values of K and β were 3.62×10^6 m^{-2} and 80.19 m^{-1}, respectively. The presence of the carry bag increased the coefficients significantly and the corresponding values of the coefficients were 1.74×10^7 m^{-2} and 358.08 m^{-1}, respectively. These parameters were determined for a particle

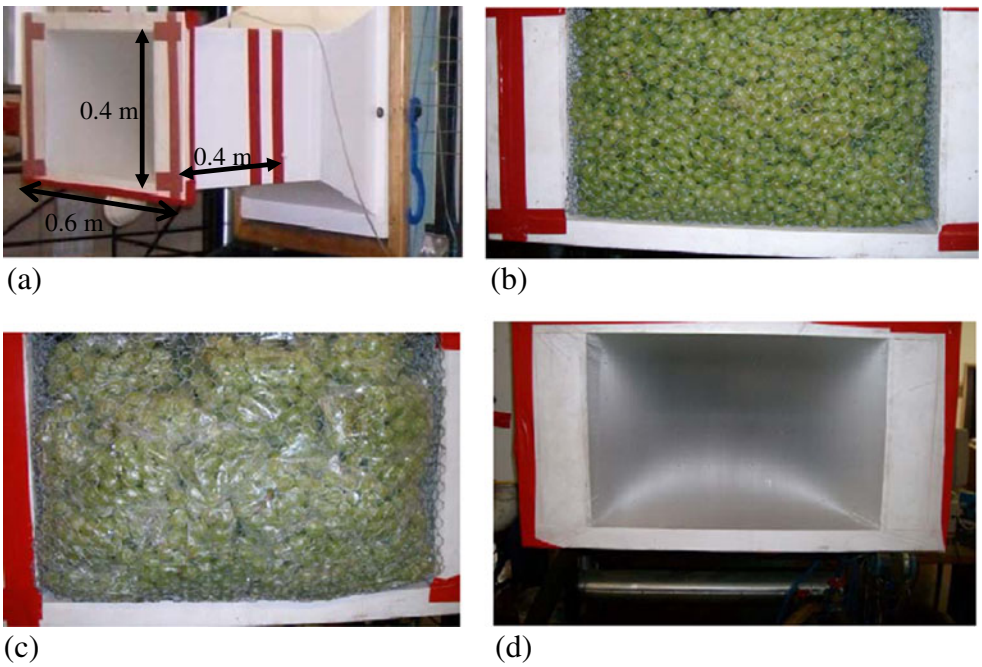

Fig.3 Wind tunnel experimental setup for airflow resistance measurement; **a** wind tunnel test section; **b** bulk of grape bunch without carry bag; **c** bulk of grape bunch with carry bag; **d** vented plastic liner

Reynolds number ($Re_p = \frac{\rho u D_p}{\mu}$) range of 63–3,347. This range corresponds to an intermediate to turbulent flow region. For flow through porous media, it is reported that $Re_p<10$, $10 \geq Re_p \leq 300$ and $Re_p>300$ distinguish laminar, intermediate and turbulent flow regimes, respectively (Eisfeld and Schnitzlein 2001). The flow in this experiment was in the range of intermediate to turbulent, but including the laminar flow region could improve the accuracy of parameter estimation.

Pressure loss coefficients of the porous jump boundary for vented plastic liners were also determined from measured data. Porous jump boundary condition is normally used to model a thin membrane with a known pressure drop characteristics. For this boundary, the pressure drop is expressed as: $\Delta p = -\left(\frac{\mu}{K}u + \beta\frac{1}{2}\rho u^2\right)t_l$, where t_l is the thickness of the liner. Pressure drop through the different vented plastic liners was measured by fixing the liner perpendicular to the airflow direction (Fig. 3d). Fan frequency range and pressure sensors used in this experiment were similar to the previous experiments on flow through bulk grape bunch and vented plastic liner. Reynolds number of the flow based on the hydraulic diameter of the tunnel was in the range of 832–9,280, the range covers laminar, intermediate and turbulent flow regions. The critical Reynolds number of channel flow is reported to be around 1,300 (Patel and Head 1969; Högberg et al. 2003). The measured pressure drop data were fitted to the above equation and corresponding values of $\frac{1}{K}$, β and liner thickness (t_l) for different vented plastic liners are given in Table 1 ($r^2 \geq 0.991$). The thicknesses of the liner were taken from Ngcobo et al. (2011).

The effect of the cooler on room airflow and humidity distribution was also included in the model. As the air passes through the finned tube heat exchanger, there is a significant pressure drop and condensation of water vapour over the cold heat exchanger surfaces. The cooler was also modelled as a porous medium; however, the Darcy term was neglected and the parameter β was calculated by taking into account losses due to wall friction, entrance and exit and acceleration/deceleration effects (Tso et al. 2006). The quadratic term dominates the pressure drop when the flow Reynolds number ($Re = \frac{\rho_a u D_c}{\mu_a}$) is much greater than 1 (Zukauskas and Ulinskas 1990; Tso et al. 2006; Verboven et al. 2006; Jacimovic et al. 2006). In this study, the *Re* of the flow through the cooling unit was 3,854.21 and corresponding value of β was 42.6 m^{-1}. The source due to the heat loss to the cooler (S_{ec}) was calculated using:

$$S_{ec} = \frac{Q_c}{V_c} = \frac{h_{hc} A_c (T_c - T_a)}{V_c} + \mathrm{LS}_{mc} \tag{8}$$

To calculate the mass source due to the condensation of water vapour on the cooler (S_{mc}) and L is the latent heat of evaporation (in Joules per kilogramme), the following equation was used:

$$S_{mc} = \frac{m_c}{V_c} = \frac{h_{mc} A_c \rho_{da} (X_{vc} - X_{va})}{V_c} \tag{9}$$

The convective mass transfer coefficient (h_{mc}) was calculated according Lewis correlation of heat and mass transfer ($h_{mc} = \frac{h_{hc}}{\rho C_p Le^{2/3}}$) (Tso et al. 2006). Where *Le* is the Lewis number and was taken as 0.95 and 1 for frosting and non-frosting condition, respectively.

The heat of respiration (S_{ep}) of the grapes was calculated using $S_{ep} = 4.599e^{0.1134T_P}$ (Becker et al. 1994). The product moisture loss was calculated using a lumped convection model, neglecting the moisture diffusion inside the product:

$$S_{mp} = h_b a_p \left(P_{vp} - P_{va}\right) \tag{10}$$

Where the P_{vp} and P_{va} are vapour pressures on the product surface and surrounding air, respectively. For thermodynamic equilibrium the surrounding air temperature approaches the product surface temperature and the vapour is assumed to follow the ideal gas law, $P_{vp} = a_w P_{sat}$ and $P_{va} = P_{sat}\left(\frac{RH}{100}\right)$. Details about the calculation of the bulk product mass transfer coefficient (h_b) can be found in 'CFD Model Formulation'. Skin mass transfer coefficient and water activity (a_w) of the grape was taken from Becker et al. (1994) and the values were 4.02×10^{-10} kg m^{-2} s^{-1} Pa^{-1} and 0.98, respectively. Average specific area ($a_p = \frac{6\phi}{D_p}$) of the grape bulk was taken as 158.21 m^2 m^{-3} (Verboven et al. 2006). The model used user defined functions to include the heat and mass transfer source terms.

Table 1 Pressure loss coefficients of the different plastic liners

Liner type (number×size (mm))	Liner thickness (μm)	1/K (m^{-2})	β (m^{-1})
0×0 (non-perforated)	20	–	–
30×2	16	6.91×10^7	2.47×10^4
54×2	16	4.81×10^7	2.17×10^4
120×2	16	4.64×10^7	1.90×10^4
36×4	16	4.09×10^7	1.85×10^4

Boundary Conditions and Simulation Procedure

The dimensions of the simulation domain were the same as the experimental cool room (Fig. 1). The fan was modelled as a fan boundary with a given pressure rise (32 Pa). This was a lumped parameter model that predicted the amount of flow through the fan, but did not take into account the detail flow behaviour and the turbulence created through the fan blades. Detail geometries of the vented carton box and pallet were explicitly modelled (Fig. 4). The product and cooler

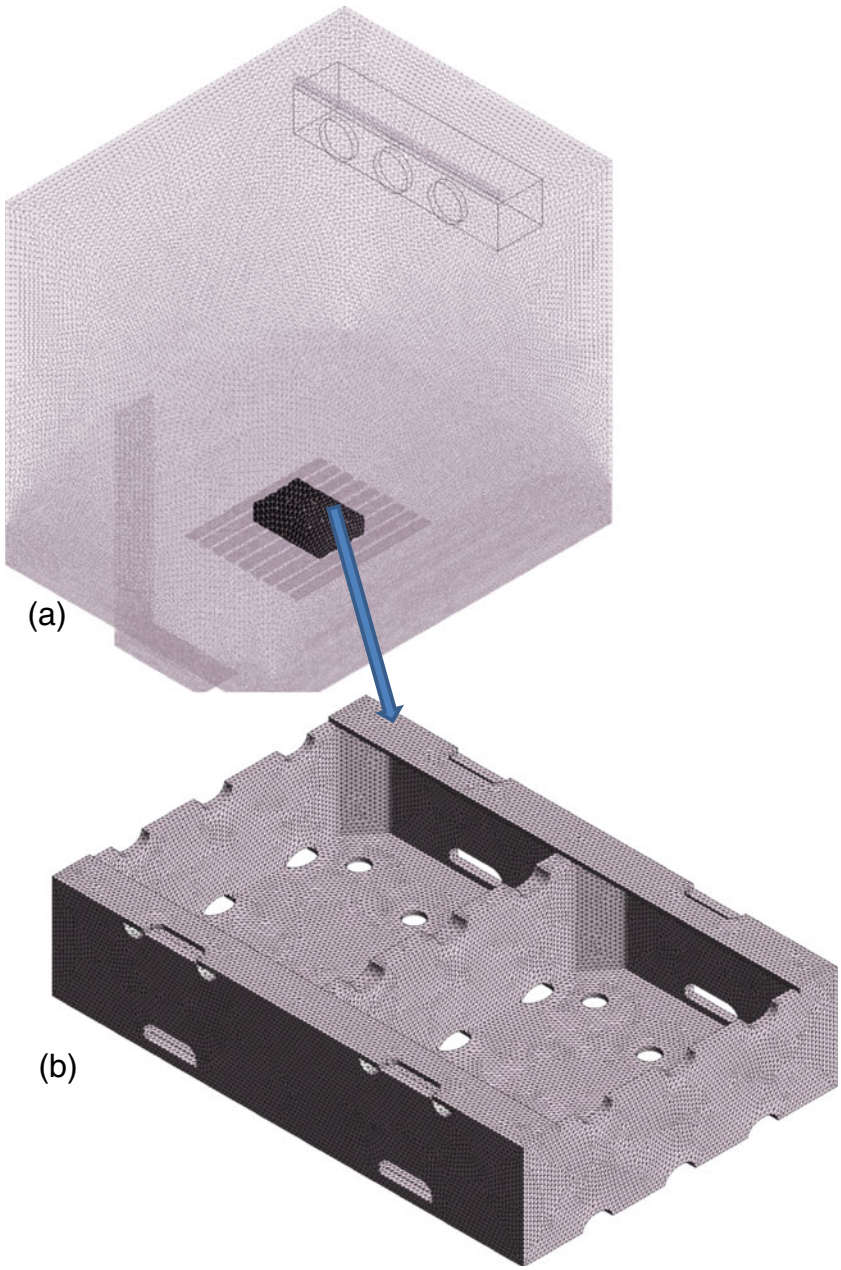

Fig. 4 Details of the geometry and computational mesh used for the model simulation; **a** whole computational domain; **b** carton box

were treated as porous medium; the determination of relevant source terms is given in 'Model Parameters Determination'. Vented liners were taken as porous jump boundaries with the corresponding loss coefficients ('Model Parameters Determination'), whereas non-perforated plastic liner was treated as a wall boundary. Moisture absorption pad and corrugated riffle sheet were also taken as wall boundaries. Condensation of water vapour on these surfaces was modelled and it occurred when the vapour pressure of the air next to wall surfaces is higher than the saturated vapour pressure. The initial cool room temperature and RH were measured and found to be 0.13 °C and 90.77 %, respectively (Temptale4 Humidity and Ambient Temperature 16000, SENSITECH, Beverly, MA, USA).

The governing equations were numerically solved using the finite volume method. The computational domain was discretised using a tetrahedral hybrid mesh (Fig. 4). The selection of the optimum mesh size was based on the size and complexity of the zones. Mesh with a maximum edge length of 0.005 and 0.01 m for box and product zones was used, respectively. The other regions were discretised using mesh with maximum edge length of 0.03 m. The mesh consisted of over 4.62×10^6 cells. This mesh size selection was made based on a mesh sensitivity study. Comparison of the calculated results (wall y^+ value, product temperature and RH) and central processing unit (CPU) time of calculation for different mesh sizes was made. Wall y^+ value is a dimensionless parameter defined by: $y^+ = \frac{\rho u_\tau y_p}{\mu}$, where u_τ is

the friction velocity, y_p is the distance from point P to the wall, ρ is fluid density and μ is fluid viscosity at point P. There was no significant change in value of the results when the mesh was less this size ($p<0.05$). The calculated y^+ values were less than 5, and that fulfilled the requirement of enhanced wall function that was used in this model. The importance of such low y^+ values on wall surfaces was also discussed by Tutar et al. (2009).

The equations were discretised using a second order upwind scheme and pressure–velocity coupling was done using a semi-implicit method for pressure-linked equations (SIMPLE) algorithm. SIMPLE algorithm uses the relationship between velocity and pressure corrections to enforce mass conservation and to get the pressure field. SIMPLE calculation is initiated with a guessed pressure field and the discretised momentum equation is solved using the guessed pressure field. A time step of 120 s and 50 iterations per time step were used. The simulation was converged to a solution with a normalised scaled residual below 10^{-4} for all equations. In normalised scaled residual analysis, the residual shows the error in the conservation equations and it is scaled using the global value, finally normalised by dividing using the maximum residual value. The residual of energy equation was converged below 10^{-7}. For most problems, normalised scaled residual value of 10^{-3} for all equations except energy and species transport equations and 10^{-6} for energy and species transport equations gives sufficient accuracy (Ansys 2010). Sensitivity of the solution to different time steps (3,600, 1,800, 600, 120 and 60 s) was assessed and no significant changes in the result were found when the time step was lower than 120 s ($p<0.05$). The calculation was done using 64-bit, Intel® Core™2 i7 CPU, 2.93 GHz, 8 Gb RAM, Windows 7 computer and the CPU time of calculation was more than 22 h.

Model Validation Experiments

Validation experiments were conducted inside experimental cold storage room (Fig. 2). The inside fruit temperature and RH of the cooling air were measured using Logtag temperature probe (LogTag Recorder Limited, Northcote, Auckland, New Zealand) and SENSITECH TempTale 4 monitor (Temptale4 Humidity and Ambient Temperature 16000, SENSITECH, Beverly, MA, USA), respectively.

'Regal' seedless grapes were obtained from the Hexriver area of the Western Cape, South Africa. The size of the grapes used was extra-large and it was assumed spherical (diameter of 20.15±0.13 mm). Cooling experiments were conducted for three packaging configurations. First, measurement was conducted with the grapes placed inside the vented carton box without the other package components (carry bag, plastic liner and SO_2 and moisture absorption pads). In the case of the second experiment, grapes were placed in carry bags and the carry bags with the grapes were packed inside the vented carton box. This experiment excluded plastic liner, SO_2 pad and moisture absorption pad. In the last case, experiment was done with all the package components included as per the commercial requirement (Fig. 1). Different plastic liners were used; these include non-perforated, 120×2 mm perforated, 54×2 mm perforated and 36×4 mm perforated. The numbers on the vented liners indicate the number and size of the holes. In all cases, the corrugated riffle sheet was placed at the bottom of the vented carton box. The cooling experiments were conducted by placing two carton boxes with the same packaging configuration adjacent to each other on a pallet. Three temperature sensors and one RH sensor were included in every carton (Fig. 5). To evaluate the effect of stacking, 30 boxes of grape were stacked on a pallet in three levels (10 boxes per level) according to the commercial guideline (Fig. 1a). The grapes were packed using 120×2 mm perforated liners. Each experiment was repeated three times.

Results and Discussion

Cooling Airflow and Temperature Distribution

The predicted airflow and temperature profiles are shown in Figs. 6 and 7, respectively. High velocity cold air that was

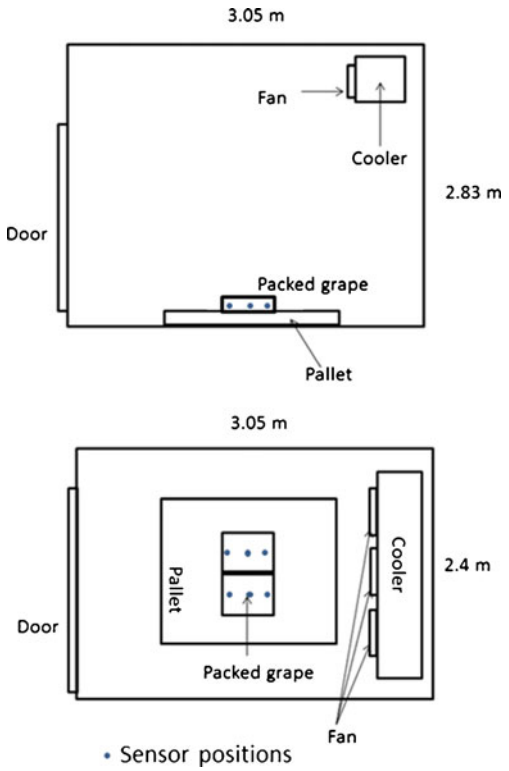

Fig. 5 Experimental setup inside the cold storage room; *circles* position of sensors

exited from the fan was attached to the ceiling of the cold room, went downward to door side of the room, cooled the product and circulated back to the cooler. Large portion of the cooling air was flowing over the surface of the packed product (Fig. 6). Only some portion of the cooling air was able to pass through the vent holes of the box. Due to the high flow resistance, the flow of cooling air through the plastic liner into the bulk of the grapes was very limited. The flow through the non-perforated liner was completely blocked, but in the case of perforated liner there was a very small amount of air that passed through it. The velocity of the air within the package was very small, and it was moving as a result of the buoyancy force. For instance, in the case of non-perforated liner the average velocity inside the bulk grape after 12 h of cooling time was 0.0041 ms^{-1}.

The cooling process progressed from the surfaces that were exposed to the flowing cold air to the central region of the package (Fig. 7); product temperature was expressed as a dimensionless temperature (θ) ($\theta = \frac{T-T_a}{T_i-T_a}$), where T_a and T_i are cooling air and initial product temperature, respectively (Dincer 1995b). The half and the seven eighth cooling time correspond to a θ value of 0.5 and 0.125, respectively. Half

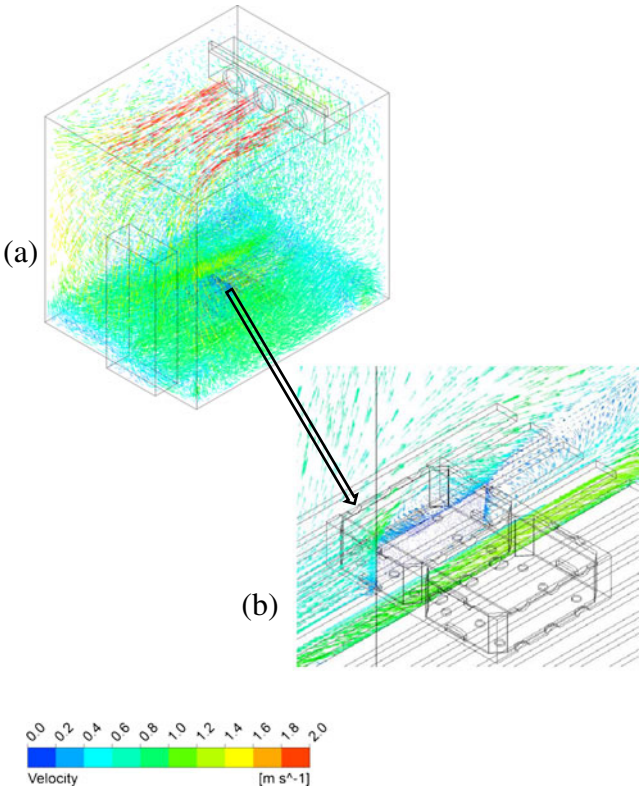

Fig. 6 Predicted airflow profile inside the cold storage room loaded with pallet with two grape boxes packed with non-perforated plastic liner; **a** air velocity vector throughout the room; **b** airflow contour on a plane that passes through the grape package

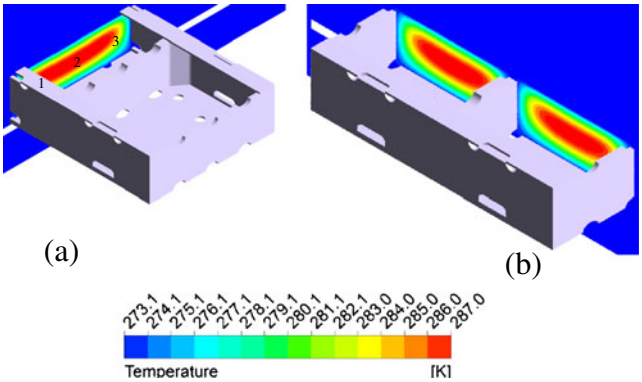

Fig. 7 Predicted temperature distribution inside the grape package, packed with non-perforated plastic liner after 6 h of cooling from the initial temperature of 21 °C (294.15 K); **a** along the length of the box and **b** along the width of the box

and seven eighth cooling times of the side that was exposed to high velocity cold air (position 1 in Fig. 7) were 5.08 and 17.42 h, compared with the 7.78 and 23.67 h for centre region of the package (position 2 in Fig. 7), respectively. Gowda et al. (1997) reported an identical trend in a parametric study conducted on forced air pre-cooling of spherical food in bulk. The layer that was nearest to the entry of the cooling air, cooled earliest whereas, the layer that was farthest from the entry point had the highest temperature. The measured and predicted results were in agreement (Fig. 8). Inside the package, conduction was the dominant mode of heat transfer. This was due to relatively low flow of cooling air into the package. During cooling of stack of products with a low velocity air (≤0.20 ms^{-1}), conduction between products

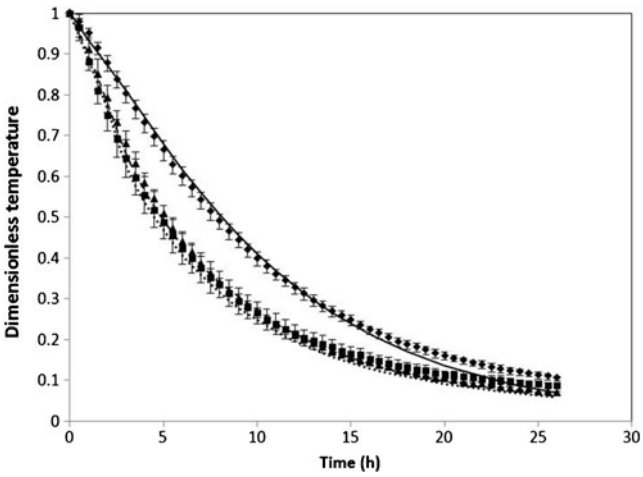

Fig. 8 Measured and predicted product temperature during cooling at different positions within the grape package; position 1, measured (*squares*) and predicted (*dotted line*); position 2, measured (*diamonds*) and predicted (*solid line*); and position 3, measured (*triangles*) and predicted (*dashed line*); the positions are shown in Fig. 7

can be the same order of magnitude as convection (Amara et al. 2004). This result shows that for such packaging system a simple diffusion model combined with the appropriate boundary condition may give reasonable accuracy with lower computational cost. However, in complex flow system like room air cooling, determining the correct boundary condition is challenging. Boundary conditions over the package are spatially highly variable and depend on several factors. For instance, in this study the heat transfer coefficients between front and back and top and bottom sides were different and there was also difference between different positions within the same side. The convective heat transfer coefficient over the surface of the package was in the range of 1.2 to 23.4 Wm^{-2} $°C^{-1}$. Boundary conditions for different design (box and liner) and operating condition (airflow rate, stacking, etc) are different. Experimental determination of boundary condition for each of the cases at high spatial resolution is time consuming, difficult and expensive. Cool room model that takes into account all the geometric, airflow, heat and mass transfer details is an alternative to predict the boundary condition in relatively easy and cheaper way. Such full-scale refrigerated system models have been validated and used in number of applications and found to be reasonably accurate (Hoang et al. 2000; Moureh and Flick 2004; Moureh and Flick 2004; Nahor et al. 2005; Mirade and Picgirard 2006; Chourasia and Goswami 2007; Delele et al. 2009a, b). The full scale model can be used to develop database of boundary conditions for different design and operating parameters that can be incorporated in the development of simplified diffusion model of grape packaging system.

Effect of Package Components on Heat and Mass Transfer During Cooling and Storage

The effects of bunch carry bags and plastic liners were analysed on heat and mass transfer. Bunch carry bag and plastic liners significantly affected the cooling time (Fig. 9). Placing the grape bunches in carry bag increased the half cooling time by 61.09 % from 1.8 to 2.9 h while the seven eighth cooling time increased by 97.34 % from 3.7 to 7.3 h. Nelson (1978) conducted an experimental study on the cooling of paper wrapped grape bunch cluster and reported a similar reduction in cooling rate as a result the chimney wrap. However, the addition of the carry bag did not affect the RH of the cooling air around the product which was 90.77 % on the average. RH was calculated by taking the ratio of the partial pressure of water vapour actually present in the air–water vapour mixture to the saturation pressure of water vapour at the mixture temperature. ANSYS

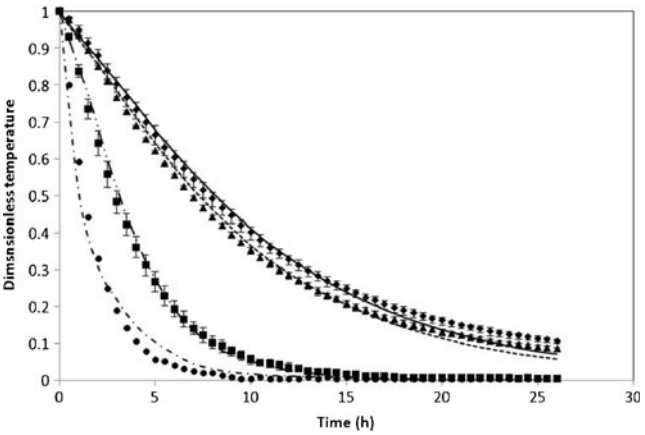

Fig. 9 Measured and predicted temperatures at the centre of the grape package for different liner and packaging systems at the centre of the package (position 2 in Fig. 7); non-perforated liner, measured (*diamonds*) **and predicted (***solid line***); perforated liner (120×2 mm), predicted (***dashed line***) and measured (***triangles***); no liner with carry bag, measured (***squares***), predicted (***broken line***); grape bulk without carry bag and liner, measured (***circles***) and predicted (***dashed–dotted line***)**

FLUENT calculates the saturation vapour pressure (p_{sat}) using: $\ln\left(\frac{p_{sat}}{p_c}\right) = \left(\frac{T_c}{T} - 1\right) \times \sum_{i=1}^{8} F_i\left[\alpha\left(T - T_p\right)\right]^{i-1}$ (Ansys 2010; Reynolds 1979). Where $p_c = 22.089$ MPa, $T_c = 647.283$ K, $F_1 = -7.4192$, $F_2 = 2.9721$, $F_3 = -1.1553 \times 10^{-1}$, $F_4 = 8.6856 \times 10^{-3}$, $F_5 = 1.0941 \times 10^{-3}$, $F_6 = -4.3999 \times 10^{-3}$, $F_7 = 2.5207 \times 10^{-3}$, $F_8 = -5.2187 \times 10^{-4}$, $\alpha = 0.01$ $T_p = 338.15$ K. Enclosing grape bunch loaded carry bags inside non-perforated liners increased the half cooling and the seven eighth cooling time by 168.90 and 185.22 %, respectively (Fig. 9). Nelson (1978, 1985) and Gentry and Nelson (1964) conducted an experimental study on the effect of plastic liner and observed a similar reduction in cooling rate. Covering with 120×2 mm perforated plastic liner increased half and seven eighth cooling time by 137.81 and 175.70 %, respectively. Relative to the non-perforated liner, perforated liners decreased half and seven eighth cooling time by 11.46 and 11.41 %, respectively. The improvement in cooling rate as a result of liner perforation was not that big. This could be due to suboptimal vent parameters (size, number and position) and blockage of the vents by the product and the box surfaces. This result shows that in order to get the required improvement in cooling rate optimal design and operation of perforated liner is necessary. The velocity of the air inside the package was a little bit higher than the non-perforated liner; for instance, after 12 h of cooling time the air velocity 0.0059 ms^{-1} compared with 0.0041 ms^{-1}. The difference in cooling time between the different perforated plastic liners used

in this study (120×2, 36×4 and 54×2 mm) was not significant ($p<0.05$).

The effect of the non-perforated liner on maintaining high RH inside the package was very vital (Fig. 10). Predicted total moisture loss from grapes that were packed with non-perforated liner and cooled from an initial temperature of 21 °C to a storage temperature of −0.5 °C and handled at this temperature for 1 month was only 0.18 %. After cooling time of 8.2 h, the air inside the packed system was completely saturated (RH=100 %) and resulted vapour condensation. This phenomenon was also reported by Ngcobo et al. (2011) and Lichter et al. (2011). For perforated liners, the maximum RH that was attainable inside the package was the RH of the cooling air. In this case, after pre-cooling and 1-month storage at −0.5 °C, the predicted total moisture was 1.23 %. This results show that the perforation of plastic liners mainly affect the moisture transfer. Non-perforated liner was able to minimise the moisture loss. The lower moisture loss could help to minimise weight loss, stem drying, browning, softening and shattering of berries, but the high rate of condensation inside the package could enhance microbial growth and SO_2 injury. Previous studies described the advantage of plastic liner in minimising grape moisture loss and in maintaining quality (Lichter et al. 2011, 2008; Nelson and Ahmedullah 1976; Costa et al. 2011; Crisosto et al. 1994; Ngcobo et al. 2011). Crisosto et al. (1994) conducted a moisture loss study on Thompson Seedless grapes with and without plastic liner. After 12 days of storage at 0–1 °C and 3 days of shelf life at 20 °C, observed moisture loss of 0.4 and 7.6 % for package with and without plastic liner, respectively. In the same study, after 28 days of shipment at 0–1 °C and 3 days of shelf life at 20 °C, for package with perforated liner moisture loss of 0.4 % was reported whereas, no moisture loss was observed for non-perforated liner. The experimental study conducted by Ngcobo et al. (2011) reported moisture loss of 0.70 and 1.80 % after 30 days of storage at 0.5 °C for table grapes packaged with non-perforated and perforated liner, respectively. Design of liner that is capable of minimising grape moisture loss but prevent the accumulation of the condensed water inside the package is very vital (Lichter et al. 2011).

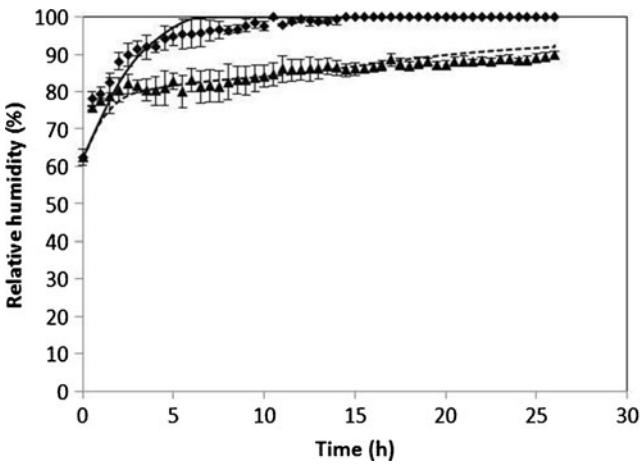

Fig. 10 Measured and predicted RH inside grape package packed using plastic liners; non-perorated, measured (*diamonds*) and predicted (*solid line*) and perforated liner (120×2 mm), predicted (*dashed line*) measured (*triangles*)

Previous studies focused mainly on experimental evaluation of the effects of table grape liner vents on moisture loss and moisture condensation (Ngcobo et al. 2011). The vents on a plastic liner are expected to increase the cooling rate and to decrease the amount of condensation inside the package. Results obtained in the present study showed that vents only minimised condensation inside the package and increased moisture loss; however, the effect of liner vents on fruit cooling rate was relatively small. These results highlight the need to design liner vents that are capable of maximising fruit cooling rate with minimum moisture loss. The developed CFD model can be used to optimise vent design of table grape liners, thereby reducing the cost of experimental studies.

Effect of Product Stacking on Heat and Mass Transfer During Cooling and Storage

The airflow pattern and temperature distribution within and around the stack of grape packages is shown in Fig. 11. Only some portion of the cooling air appeared to penetrate the stack through the gaps between the boxes (Fig. 11a). The hottest region was located near the central region of the stack. The region that was located near the entry of the cooling air had faster cooling rate than the interior region (Fig 11b and c). The half and seven eighth cooling time at centre of the stack was 23.19 and 63.92 h, respectively. These cooling times were 193.42 and 204.09 % higher than the corresponding cooling time of the two boxes mentioned in ‘Effect of Package Components on Heat and Mass Transfer During Cooling and Storage’, respectively. Due to the perforated liner (120×2 mm) that was used in this study, the maximum RH attained inside the packed boxes was the same as the RH of the cooling air. To attain maximum RH at the hottest spot in the stack, a cooling time of 87.64 h was needed, which was an increase of 212.90 % relative to the case of the two boxes that was mentioned above. The predicted total moisture loss of the stack that was cooled from an initial temperature of 21 °C to a storage temperature of −0.5 °C and stored at this temperature for a period of 1 month was 1.88 %. This moisture loss was 34.6 % higher compared with the two boxes. This result indicated that stacking of the package on the pallet during handling affected the heat and mass transfer characteristics of the package. Nelson (1978) conducted an experiment to study the pre-cooling of grape package and observed significant effect of

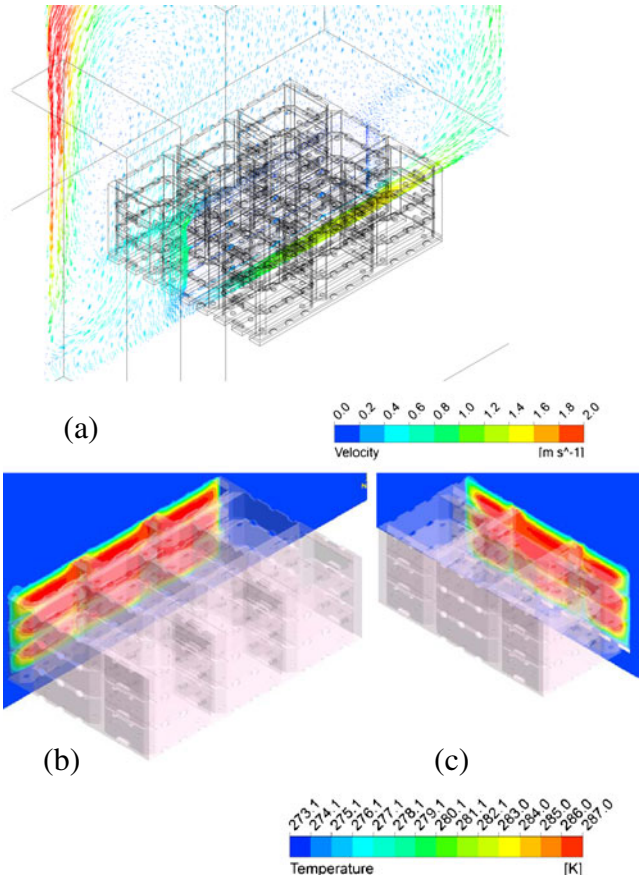

Fig. 11 Predicted airflow and temperature profiles within and around stack of grape packages, after 6 h of cooling from the initial temperature of 21 °C (294.15 K); **a** airflow vectors; **b** temperature along the length of the stack; **c** temperature along the width of the stack

number and arrangement of packages on the pallet. Due to the low penetration of the cooling air to the central region of the stack, the larger the pallet the more difficult to pre-cool.

Improving the Grape Packaging and Cooling Procedure

The validated model was applied to study alternative grape packaging and cooling procedures. First, bulk grape bunches were placed inside the vented box and cooled to storage temperature. As soon as the storage temperature was attained grape bunches were placed inside the carry bag and plastic liner. In this way of cooling, the seven eighth cooling time was reduced by 78.11 %, showing that this approach could help to reduce the total energy consumption of system. However, in this cooling procedure the RH inside the package was relatively small. During packing with perforated plastic liner the RH throughout the storage period was the same as the RH of the cooling air. However, in the case of non-perforated liner there was a slight increase of RH inside the package (2.12 %) during one month storage period. Relative to the standard way of packaging and cooling, this method minimised the cooling energy and avoided the moisture condensation. The total energy consumption increases with pre-cooling time (Thompson et al. 2010). However, the total moisture loss was relatively increased. After pre-cooling and 1-month storage at −0.5 °C, calculated total moisture loss of 0.57 and 1.39 % was observed for non-perforated and perforated liner, respectively.

In the second case, grape bunches were covered with carry bags and placed inside vented box, followed by cooling to the storage temperature. When it reached the storage temperature it was covered by plastic liner. In this case, the seven eighth cooling time was reduced by 64.82 %. The behaviour of the RH inside the package was the same as the first case. In terms of energy saving, this method of cooling was worse than the first case. However, the degree of moisture loss and condensation was not significantly different from the first case ($p<0.05$).

The third case studied the effect of cooling with high RH air. In this study the grapes were packed and cooled in a standard way but the cooling air had relatively high RH (96 %). The grapes were packed with perforated liner. With this cooling and storage method, it was possible to minimise the moisture loss by 71.16 %, but its effect on cooling rate was not significant ($p<0.05$). It is known that high RH cooling air minimises moisture loss by minimising the vapour pressure deficit between the grape surface and the cooling air (Gentry and Nelson 1964; Nelson 1978; Lichter et al. 2011). This high level of RH can be attained by using an external humidifier. In addition to maintaining the required high RH, a humidifier that works with water misting can even increase the cooling rate by evaporative cooling effect (Delele et al. 2009a).

In the last case, the grape bunches were covered with carry bags and placed inside a vented box and cooled to the half cooling time. After reaching the half cooling time the grapes inside the carry bag were covered with plastic liner and the cooling of the package was continued up to the storage temperature. In this scenario, the seventh eight cooling time was reduced by 41.60 %. For non-perforated plastic liner, it was possible to get high RH (97.15 %) inside the package with no condensation whereas, for perforated liners the RH inside the package was the same as the RH of the cooling air. The calculated total moisture loss after pre-cooling and 1-month storage at 0.5 °C was 0.34 and 1.31 % for non-perforated and perforated liner, respectively.

Conclusions

Table grapes are normally packed in multilayer packages. For efficient postharvest handling and cooling of table grapes, optimal design, packing and operation of the package are very important. The airflow, heat and mass transfer

characteristics in and around table grape packaging system were studied using CFD model. The model was validated using experimental results.

The effects of different package components on airflow, heat and mass transfer processes were studied. The validated model was applied to evaluate alternative packaging and cooling procedures. The presence of bunch carry bag and plastic liner affects the cooling rate of grapes. The contribution of plastic liner in reducing the cooling rate of packed grapes was higher than the other package components. Non-perforated liner produced the highest RH inside the package that gave the lowest moisture loss but the highest condensation. Pre-cooling of table grape bunches with and without carry bag before covering it with plastic liner reduced the cooling rate significantly, up to 78.11 %. For perforated liner, the use of high RH (96 %) cooling air compared with 90.77 % minimised the moisture loss by 71.16 %. The cooling airflow pattern, cooling rate and moisture loss were also affected by the stacking of the product over the pallet. The result demonstrated the applicability of CFD models to determine the optimum table grape package design and handling that gives the maximum cooling rate with minimum water condensation and moisture loss. The approach followed in this study can be applied in the optimisation of other agricultural product packaging system design and handling. However, these models must include the appropriate system geometry, air supply properties and product physiochemical properties.

Acknowledgements This work is based upon research supported by the South African Research Chairs Initiative of the Department of Science and Technology and National Research Foundation. The financial support of the South African Postharvest Innovation Programme through the award of research grant on 'Packaging of the Future' project is acknowledged. The authors are grateful to Mr. Cobus Zietsman for his technical support with the wind tunnel experiment and to Ms. Nazneen Ebrahim for support in the postharvest technology laboratory. We thank the anonymous reviewers for their valuable comments and feedback.

References

Acevedo, C., Sánchez, E., & Young, M. E. (2007). Heat and mass transfer coefficients for natural convection in fruit packages. *Journal of Food Engineering, 80*, 655–661.

Alvarez, G., & Flick, D. (1999). Analysis of heterogeneous cooling of agricultural products inside bines. Part I: aerodynamic study. *Journal of Food Engineering, 39*(3), 227–237.

Alvarez, G., Bournet, P. E., & Flick, D. (2003). Two-dimensional simulation of turbulent flow and transfer through stacked spheres. *International Journal of Heat and Mass Transfer, 46*, 2459–2469.

Amara, S. B., Laguerre, O., & Flick, D. (2004). Experimental study of convective heat transfer during cooling with low air velocity in a stack of objects. *International Journal of Thermal Sciences, 43*, 1213–1221.

ANSYS (2010). ANSYS FLUENT 13.0 users guide. ANSYS, Inc., Canonsburg, PA, USA.

Antohe, B. V., & Lage, J. L. (1997). A general two-equation macroscopic turbulence model for incompressible flow in porous medium. *International Journal of Heat and Mass Transfer, 40*(13), 3013–3024.

Becker, B. R., Misra, A., & Fricke B. A. (1994). A computer algorithm for determining the moisture loss and latent heat load in the bulk storage of fruits and vegetables. Final report (project 777-RP), ASHRAE, Atlanta, USA.

Bingol, G., Pan, Z., Roberts, J. S., Devres, Y. O., & Balaban, M. O. (2008). Mathematical modelling of microwave-assisted convective heating and drying of grapes. *International Journal of Agricultural and Biological Engineering, 1*(2), 46–54.

Bird, R., Stewart, W., & Lightfoot, E. (2002). *Transport phenomena* (2nd ed.). New York: Wiley.

Caleb, O. J., Opara, U. L., & Witthuhn, C. R. (2011). Modified atmosphere packaging of pomegranate fruit and arils: a review. *Food and Bioprocess Technology.* doi:10.1007/s11947-011-0525-7.

Carson, J. K. (2006). Review of effective thermal conductivity models for foods. *International Journal of Refrigeration, 29*, 958–967.

Chau, K., Gaffney, J., Baird, C., & Church, G. (1985). Resistance to air flow of oranges in bulk and in cartons. *Transactions of ASAE, 28* (6), 2083–2088.

Chourasia, M. K., & Goswami, T. K. (2007). CFD simulation of effects of operating parameters and product on heat transfer and moisture loss in the stack of bagged potatoes. *Journal of Food Engineering, 80*(3), 947–960.

Costa, C., Lucera, A., Conte, A., Mastromatteo, M., Speranza, B., Antonacci, A., & Del Nobile, M. A. (2011). Effects of passive and active modified atmosphere packaging conditions on ready-to-eat table grape. *Journal of Food Engineering, 102*, 115–121.

Crisosto, C., Smilanick, J., Dokoozlian, N., & Luvis D. A. (1994). Maintaining table grape post-harvest quality for long distant markets. International Symposium on Table Grape Production, California, USA, 28–29 June 2004. American Society for Enology and Viticulture, pp 195–199.

Crisosto, C., Smilanick, J., & Dokoozlian, N. (2001). Table grapes suffer water loss, stem browning during cooling delays. *California Agriculturae, 55*, 39–42.

de Castro, L. R., Vigneault, C., & Cortez, L. A. B. (2004). Container opening design for horticultural produce cooling efficiency. *Journal of Food, Agriculture and Environment, 2* (1), 135–140.

de Paula, R., Colet, R., de Oliveira, D., Valduga, E., & Treichel, H. (2011). Assessment of different packaging structures in the stability of frozen fresh Brazilian Toscana sausage. *Food and Bioprocess Technology, 4*(3), 481–485.

Delele, M. A., Schenk, A., Tijskens, E., Ramon, H., Nicolaï, B. M., & Verboven, P. (2009). Optimization of the humidification of cold stores by pressurized water atomizers based on a multiscale CFD model. *Journal of Food Engineering, 91*(2), 228–239.

Delele, M. A., Schenk, A., Ramon, H., Nicolaï, B. M., & Verboven, P. (2009). Evaluation of a chicory root cold store humidification system using computational fluid dynamics. *Journal of Food Engineering, 94*(1), 110–121.

Delele, M. A., Vorstermans, B., Creemers, P., Tsige, A. A., Tijskens, E., Schenk, A., Opara, U. L., Nicolaï, B. M., & Verboven, P. (2012). Investigating the performance of thermonebulisation fungicide fogging system for loaded fruit storage room using CFD model. *Journal of Food Engineering, 109*, 87–97.

Dincer, I. (1995a). Determination of heat-transfer coefficients for cylindrical products exposed to forced-air cooling. *International Journal of Energy Research, 19*(5), 451–459.

Dincer, I. (1995b). Air flow precooling of individual grapes. *Journal of Food Engineering, 26*, 243–249.

Eisfeld, B., & Schnitzlein, K. (2001). The influence of confining walls on pressure drop in packed beds. *Chemical Engineering Science, 56*, 4321–4329.

Ferrua, M. J., & Singh, R. P. (2009). Modeling the forced-air cooling process of fresh strawberry packages, Part III: experimental validation of the energy model. *International Journal of Refrigeration, 32*(2), 359–368.

Frederick, R. L., & Comunian, F. (1994). Air-cooling characteristics of simulated grape packages. *International Communications in Heat and Mass Transfer, 21*(3), 447–458.

Gentry, J. P., & Nelson, K. E. (1964). Conduction cooling of table grapes. *American Journal of Enology and Viticulture, 15*(1), 41–46.

Gowda, B. S., Narasimham, G. S. V. L., & Murthy, M. V. K. (1997). Forced-air precooling of spherical foods in bulk: a parametric study. *International Journal of Heat and Fluid Flow, 18*, 613–624.

Hoang, M. L., Verboven, P., De Baerdemaeker, J., & Nicolaï, B. M. (2000). Analysis of air flow in a cold store by means of computational fluid dynamics. *International Journal of Refrigeration, 23*, 127–140.

Högberg, M., Bewley, T. R., & Henningson, D. S. (2003). Linear feedback control and estimation of transition in plane channel flow. *Journal of Fluid Mechanics, 481*, 149–175.

Jacimovic, B. M., Genic, S. B., & Latinovic, B. R. (2006). Research on the air pressure drop in plate finned tube heat exchangers. *International Journal of Refrigeration, 29*, 1138–1143.

Laguerre, O., Ben Amara, S., Alvarez, G., & Flick, D. (2008). Transient heat transfer by free convection in a packed bed of spheres: comparison between two modelling approaches and experimental results. *Applied Thermal Engineering 28*, 14–24.

Lichter, A., Kaplunov, T., & Lurie, S. (2008). Evaluation of table grape storage in boxes with sulfur dioxide-releasing pads with either an internal plastic liner or external wrap. *HortTechnology, 18*, 206–214.

Lichter, A., Kaplunov, T., Zutahy, Y., Daus, A., Alchanatis, V., Ostrovsky, V., & Lurie, S. (2011). Physical and visual properties of grape rachis as affected by water vapour pressure deficit. *Postharvest Biology and Technology, 59*, 25–33.

Mirade, P. S., & Picgirard, L. (2006). Improvement of ventilation homogeneity in an industrial batch-type carcass chiller by CFD investigation. *Food Research International, 39*, 871–881.

Moureh, J., & Flick, D. (2004). Airflow pattern and temperature distribution in a typical refrigeration truck configuration loaded with pallets. *International Journal of Refrigeration, 27*, 464–474.

Nahor, H. B., Hoang, M. L., Verboven, P., Baelmans, M., & Nicolaï, B. M. (2005). CFD model of the airflow, heat and mass transfer in cooling stores. *International Journal of Refrigeration, 28*, 368–380.

Nakayama, A., & Kuwahara, F. (1999). A macroscopic turbulence model for flow in a porous medium. *Journal of Fluids Engineering-Transactions of the ASME, 121*, 427–433.

Nelson, K. E. (1978). Pre-cooling-its significance to the market quality of table grapes. *International Journal of Refrigeration, 1*(4), 207–215.

Nelson, K. E. (1985). *Harvesting and handling California table grapes for market. University of California Bulletin No. 1913* (p. 72). Oakland: DANR Publications.

Nelson, K. E., & Ahmedullah, M. (1976). Packaging and decay-control systems for storage and transit of table grapes for export. *American Journal of Enology and Viticulture, 27*(2), 74–79.

Ngcobo, M. E. K., Opara, U. L., & Thiart, G. D. (2011). Effects of packaging liners on cooling rate and quality attributes of table grape (cv. Regal Seedless). *Packaging Technology and Science*. doi:10.1002/pts.961.

Opara, U. L. (2011). From hand holes to vent holes: what's next in innovative horticultural packaging? Inaugural Lecture delivered on 2 February, Stellenbosch University, 24 pages.

Opara, L. U., & Zou, Q. (2006). Novel computational fluid dynamics simulation software for thermal design and evaluation of horticultural packaging. *International Journal of Postharvest Technology and Innovation, 1*(2), 155–169.

Opara, L. U., & Zou, Q. (2007). Sensitivity analysis of a CFD modelling system for airflow and heat transfer of fresh food packaging: inlet air flow velocity and inside-package configurations. International Journal of Food Engineering, 3(5), article 16.

Patel, V. C., & Head, R. (1969). Some observations on skin friction and velocity profiles in fully developed pipe and channel flows. *Journal of Fluid Mechanics, 38*, 181–201.

Reynolds, W. C. (1979). Thermodynamic properties in SI: Graphs, Tables, and Computational equations for 40 substances. Department of Mechanical Engineering, Stanford University, Stanford.

Tassou, S. A., & Xiang, W. (1998). Modelling the environment within a wet air-cooled vegetable store. *Journal of Food Engineering, 38*, 169–187.

Thompson, J. F., Mejia, D. C., & Singh, R. P. (2010). Energy use of commercial forced-air cooler for fruit. *Applied Engineering in Agriculture, 26*(5), 919–924.

Tsiraki, M. I., & Savvaidis, I. N. (2011). Effect of packaging and basil essential oil on the quality characteristics of whey cheese "Anthotyros". *Food and Bioprocess Technology*. doi:10.1007/s11947-011-0676-6.

Tso, C. P., Cheng, Y. C., & Lai, A. C. K. (2006). An improved model for predicting performance of finned tube heat exchanger under frosting condition with frost thickness variation along fin. *Applied Thermal Engineering, 26*, 111–120.

Tutar, M., Erdogdu, F., & Toka, B. (2009). Computational modeling of airflow patterns and heat transfer prediction through stacked layers products in a vented box during cooling. *International Journal of Refrigeration, 32*, 295–306.

van der Sman, R. G. M. (2002). Prediction of air flow through a vented box by the Darcy–Forchheimer equation. *Journal of Food Engineering, 55*(1), 49–57.

van der Sman, R. G. M. (2008). Scale analysis and integral approximation applied to heat and mass transfer in packed beds. *Journal of Food Engineering, 85*, 243–251.

Verboven, P., Flick, D., Nicolaï, B. M., & Alvarez, G. (2006). Modelling transport phenomena in refrigerated food bulks, packages and stacks: basics and advances. *International Journal of Refrigeration, 29*, 985–997.

Versteeg, H. K., & Malalasekera, W. (1995). *An introduction to computational fluid dynamics—the finite volume method*. New York: Wiley.

Vigneault, C., & de Castro, L. R. (2005). Produce-simulator property evaluation for indirect airflow distribution measurement through horticultural crop package. *Journal of Food, Agriculture and Environment, 3*(2), 67–72.

Vigneault, C., & Goyette, B. (2002). Design of plastic container opening to optimize forced-air precooling of fruits and vegetables. *Applied Engineering in Agriculture, 18*(1), 73–76.

Wakao, N., & Kaguei, S. (1982). *Heat and mass transfer in packed beds* (pp. 243–295). New York: Gordon & Breach.

Wilcox, D. C. (2000). *Turbulence modeling for CFD* (2nd ed.). La Canada: DCW Industries, Inc.

Xu, Y., & Burfoot, D. (1999). Simulating the bulk storage of food stuffs. *Journal of Food Engineering, 39*, 23–29.

Zou, Q., Opara, L. U., & McKibbin, R. (2006). A CFD modeling system for airflow and heat transfer in ventilated packaging for fresh foods: II. Computational solution, software development, and model testing. *Journal of Food Engineering, 77*(4), 1048–1058.

Zukauskas, A., & Ulinskas, R. (1990). Banks of plain and finned tubes. In G. F. Hewitt (Ed.), *Handbook of heat exchanger design* (pp. 2.2.4-1–2.2.4-17). London: Hemisphere.